

Intracavity frequency converted Raman laser producing 10 deep blue to cyan emission lines with up to 0.94 W output power

Dimitri Geskus,¹ Jonas Jakutis-Neto,² Helen M. Pask,³ and Niklaus U. Wetter^{1,*}

¹Centro de Lasers e Aplicações, IPEN/SP, Av. Prof. Lineu Preses, 2242 São Paulo, SP, Brazil

²Instituto de Estudos Avançados, IEAv-DCTA, Trevo Cel. Av. José A. A. do Amarante, 1, Putim 12228-001 São José dos Campos, SP, Brazil

³MQ Photonics, Department of Physics and Astronomy, Macquarie University, Sydney, NSW 2109, Australia

*Corresponding author: nuwetter@ipen.br

Received August 7, 2014; revised October 15, 2014; accepted November 4, 2014;
posted November 5, 2014 (Doc. ID 220618); published December 5, 2014

Here we report 10 laser emission lines in the attractive deep blue to cyan spectral region from an intracavity frequency doubled Raman laser. The fundamental laser field that drives the Raman laser is based on the three-level transition of Nd:YLF. A maximum extracted quasi-continuous wave (qcw) output power of 0.94 W is achieved in the deep blue to cyan spectral regime. © 2014 Optical Society of America

OCIS codes: (140.3530) Lasers, neodymium; (140.3550) Lasers, Raman; (190.2620) Harmonic generation and mixing.
<http://dx.doi.org/10.1364/OL.39.006799>

Many “hard to reach” wavelengths in the near-infrared and visible spectral regions can efficiently be reached using wavelength agile, all solid-state intracavity frequency converted Raman lasers [1,2]. By making use of a high-*Q* cavity, the highly enhanced intracavity fundamental field provides strong stimulated Raman scattering (SRS), allowing continuous wave (cw) SRS laser operation [3]. In addition, intracavity sum frequency generation (SFG) and second harmonic generation (SHG) have been reported, resulting in laser output in the yellow–orange–red spectral region [4–6]. Continuous improvements in crystal quality and coating technologies have been of paramount importance for providing optical to optical (diode pump to visible) efficiencies in excess of 20% [4].

Recent achievements in intracavity Raman laser technology using the $^4F_{3/2}$ – $^4I_{9/2}$ three-level laser transition of Nd:YLiF₄ (Nd:YLF) resulted in laser operation at three different lines in the wavelength region between 908 and 990 nm [7], opening the way for Raman lasers in the blue spectral range. Here we present for the first time, to the best of our knowledge, an intracavity frequency converted Raman laser that can emit 10 lines in the deep blue to cyan (452–495 nm) spectral range, achieved by an SFG of a fundamental and/or a Stokes lines. These 10 blue emission lines demonstrate the wavelength agile character of Raman lasers. Moreover, the laser can be configured such that an operator can easily switch between a set of three blue wavelengths, e.g., 454, 474, and 495 nm, simply by adjusting the angle of the LBO crystal. This wavelength agility could be extended further by tailoring the Raman shift by appropriate selection of Raman transition and/or Raman crystal to generate discrete wavelengths across a narrower or broader spectral region. The blue laser reported here offers a physically simple and cost-effective approach to generating blue laser output which could complement established sources such as argon ion lasers, optically-pumped semiconductor lasers (OPSLs) [8–10], and optical parametric oscillators (OPOs) [11].

Our concept for obtaining 10 blue lines from a relatively straightforward laser arrangement is shown in

Fig. 1. Nd:YLF was selected as the laser crystal because of its short operating wavelengths, relatively weak thermal lensing, the spacing of ground state energy levels which leads to moderately-low reabsorption loss, and its birefringence, which leads to polarized output at the two wavelengths of 903 and 908 nm. KGW was selected as the Raman-active crystal because of its moderately high Raman gain, weak thermal lensing, and its offering of two Raman shifts of 768 and 901 cm^{-1} , and therefore four possible first Stokes wavelengths: 970, 976, 983, and 990 nm. The further incorporation of SHG and SFG in a crystal such as LBO leads to the 10 wavelengths spanning 452–495 nm; see Fig. 2.

A linear cavity approximately 11 cm long was used, formed by two concave (ROC = 50 mm) mirrors with high reflectivity, $R > 99.9$ at 903–908 nm and $R > 99.99$ at 970–990 nm, to efficiently resonate both the laser fundamental and Raman-shifted fields inside the cavity (see Fig. 1).

The laser crystal was a 3 mm long Nd(0.7%):YLF crystal, the length and doping concentration selected to enable the pump transition to be near-saturation absorbing 46% of the pump light under non-lasing conditions, thereby reducing reabsorption losses for the laser transition. A fiber coupled laser diode at 797 nm was used as the pump source, and was operated in qcw mode with a duty cycle of 1.7% at a 25 Hz repetition rate. The output of the fiber focused to a spot radius of 100 μm into the

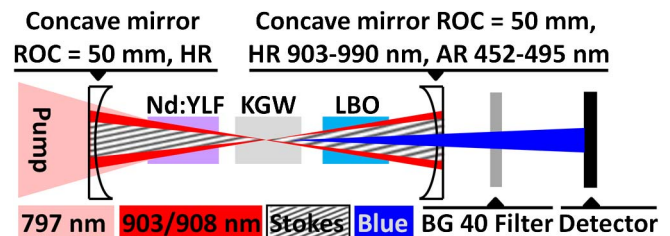


Fig. 1. Schematic of the laser setup, based on a fundamental wavelength of 908 nm, used to generate five emission lines in the blue. Changing the fundamental laser line to 903 nm creates an additional set of five deep blue to cyan emission lines.

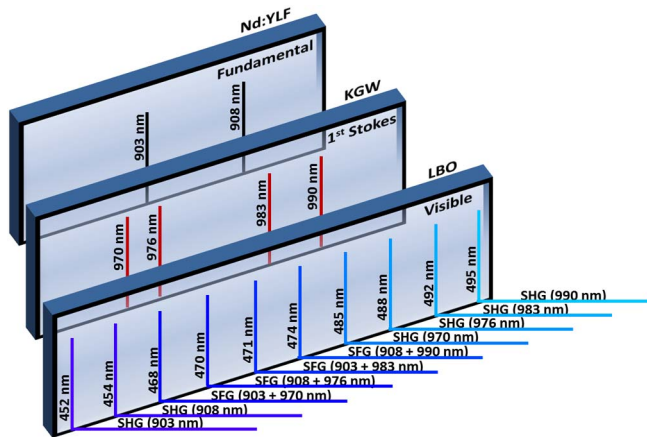


Fig. 2. Schematic of the intracavity laser processes, resulting in 10 blue spectral emission lines.

Nd:YLF crystal. A 10 mm long KGW crystal was placed in the center of the near-concentric cavity where generation of SRS benefits from the small mode size (approximately 62 μm beam radius) and thus highest intracavity intensities. The 10 mm long KGW crystal was cut for propagation along the optical N_p axis, and was AR-coated for the fundamental and Stokes wavelengths. The orientation of the KGW was adjusted by rotating it around its optical axis (N_p), so that the polarizations $E||N_m$ and $E||N_g$ could be addressed providing SRS based on the 901 and 768 cm^{-1} Stokes shift, respectively. A 5 mm long BiBO crystal and a 10 mm long LBO crystal were initially used for SFG; however the performance using the LBO crystal was clearly superior, possibly because of its better transparency at the 9XX nm wavelengths. The results presented here are based on the LBO crystal [12,13]. The LBO crystal was cut for $\theta = 90^\circ$, $\Phi = 16^\circ$ for critical phase-matching, and AR-coated for the fundamental and first Stokes wavelengths at 903–990 nm. The extraordinary polarized blue emission was coupled out of the cavity through the output coupler, which had low reflection ($R \sim 5\%$) for the deep blue to cyan wavelengths.

By changing the angle of the 10 mm long LBO crystal, three blue emission lines could be generated: SHG of the fundamental field, SFG of fundamental and Stokes laser fields, and SHG of the Stokes field. In the same way, two additional blue emission lines could be generated by rotating the KGW crystal, changing the wavelength of the Stokes field. The strong birefringent walk-off of the optical field inside the LBO crystal helped to select the polarization of the fundamental laser field. A simple tilt or translation of the concave outcoupling mirror made the cavity selective for the ordinary or the extraordinary polarization, hence forcing the polarization of the laser and the wavelength of the fundamental field to 903 nm (π) or 908 nm (σ). Note that the orientation of the LBO crystal had to be adapted to maintain extraordinary polarization of the fundamental and/or Stokes field with respect to the LBO crystal to maintain the frequency conversion to the visible. For each fundamental wavelength, five emission lines in the blue are obtained, resulting in a total of 10 deep blue to cyan spectral emission lines, as depicted in Fig. 2. Each individual spectral emission line was recorded using an Ocean Optics (HR4000)

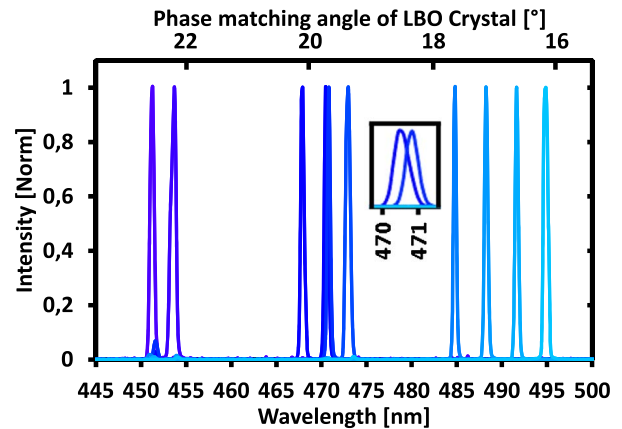


Fig. 3. Recorded emission spectra of each blue emission line. The inset shows a magnification of the 470–471 nm spectral region revealing the two emission lines in this region.

spectrophotometer with a resolution of 0.24 nm, presented in Fig. 3.

The intracavity placed LBO crystal converts the intracavity field to the visible, generating similar powers in the forward and backward propagating directions. During the characterization, only forward propagating emission was collected. Highest blue output power of 0.94 W was extracted for the 474 nm emission line in qcw mode of operation. Other strong blue emission lines at 495 and 470 nm were observed as shown in Fig. 4. Despite the larger Raman cross section of the 768 cm^{-1} Stokes shift, the corresponding emission lines at 470 and 488 nm were lower with respect to the blue emission based on the 990 cm^{-1} Stokes shift. The output power of the blue emission lines that originated from the 903 nm fundamental laser line was very low and the oscillation tended to be unstable. This is attributed to 903 nm being at the (short-wavelength) edge of the mirror reflectivity band leading to slightly larger intracavity losses at 903 nm. Higher powers can be anticipated in the future with optimized coatings. In a separate experiment, the frequency doubled fundamental laser lines were analyzed. A qcw output power of 1.08 W at 454 nm having a threshold

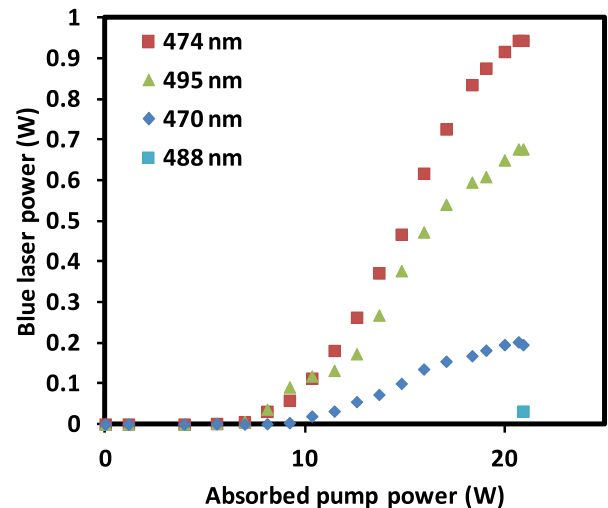


Fig. 4. SFG and SHG generated blue laser power based on the 908 nm fundamental line and its Stokes fields at 976 and 990 nm.

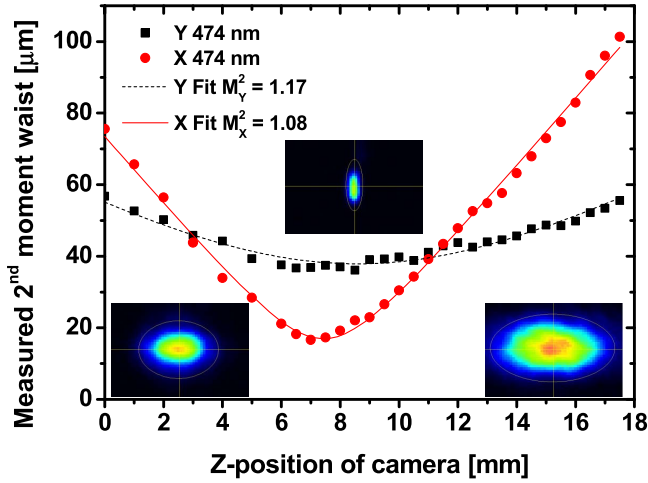


Fig. 5. M^2 measurement of the blue (474 nm) laser beam. The insets show the beam profiles recorded in far-field and focus.

of 4 W absorbed pump power and a qcw output power of 0.51 W at 452 nm with a threshold of 6 W absorbed pump power was found.

In this experiment, no KGW crystal was present in the cavity and a 10 mm long LBO-crystal cut for $\theta = 90^\circ$, $\Phi = 21.9^\circ$ was used for SHG. Although laser emission was easily observed using the original setup with the LBO crystal cut at a $\Phi = 16^\circ$ angle, the output power was compromised by the additional intracavity losses caused by the reduced performance of the AR coatings of the LBO crystal when tilted over a $\sim 10^\circ$ angle to achieve internal phase-matching angles of $\sim 22.4^\circ$. The use of temperature-tuned phase-matching is likely to be advantageous in avoiding this problem.

When analyzing the beam profile of the blue laser emission, a small walk-off is observed (see insets in Fig. 5), typical for SFG and SHG. The M^2 measurements were performed by focusing the beam of the laser emission onto a CCD camera using a biconvex lens ($f = 125$ mm) at a 28 cm distance from the cavity center. The camera was translated through the focal plane, while measuring the beam waist using the second moment beam analysis in X and Y directions. M^2 values between 1.08 and 1.17 were found for the blue emission beam in X and Y direction, respectively.

Cw laser operation at 990 nm was also achieved using a 0.28% outcoupling mirror for 990 nm and a 6 mm long Nd:YLF crystal, but without the LBO crystal inside the cavity. The cavity parameters were almost identical to the previous qcw laser experiments where the cavity length was close to the stability limit of 11 cm, having a physical length of 10.8 cm which corresponds to an optical path length of 12.1 cm. It should be pointed out that no efforts, apart from fine tuning of the cavity length, were made to optimize the cavity to compensate for thermal lensing. At 18 W of absorbed pump power the maximum extracted cw output power at 990 nm was 27 mW, which was also the fracture damage threshold of the Nd:YLF crystal. The measured cw output power of only 27 mW is much lower than the peak output power of 7.7 W obtained for the laser in the qcw operation [7]. The small cw output power can be explained by the increase of the crystal temperature in combination with the three-level nature

of the laser, affecting the laser performance significantly. In addition, an elliptical output beam shape was observed, indicating a cylindrical thermal lens. Advanced compensation of the thermal lens by a cylindrical lens [14], or adaptive optics [15], can significantly improve the performance of the Raman laser.

When the SFG was introduced into a cw laser using a 3 mm long (and therefore less absorbing) Nd:YLF crystal, a 10 mm long KGW crystal, and a 10 mm long LBO crystal inside the cavity, the output only contained 45 μ W at 474 nm. The emission was 100% modulated resulting in an irregular train of pulses with durations of the order of 100 ns. A similar pulsating behavior of the Stokes emission was observed in our earlier report [7], in which we also noticed severe spectral broadening of the Stokes and fundamental field. The underlying processes are currently being investigated, and we believe that the spectral broadening and complex laser dynamics may be related to each other and play a vital role in restricting the laser efficiency of these intracavity frequency converted Raman lasers.

The emission of 10 deep blue to cyan laser lines is reported, obtained from a Nd:YLF-KGW-LBO intracavity frequency converted Raman laser. A maximum extracted qcw power of 0.94 W at 474 nm is demonstrated for the first time, to the best of our knowledge, from such a laser. The SHG of the fundamental field delivered a maximum qcw output power of 1.08 W. Cw Raman laser operation is demonstrated, providing 27 mW of output power at 990 nm and weak (<1 mW) irregularly-pulsed blue laser emission at 474 nm. The cw laser performance shows that the quasi-three-level operation is heavily challenged by the induced heat when compared to earlier reported Watt level cw results in the yellow lime green region, using a similar laser cavity based on the four-level transition of the Nd:YLF [6]. Further studies are required to determine whether it is feasible to extract cw blue laser output from this laser system.

The 10 blue laser emission lines demonstrated here highlight the wavelength agile character of intracavity frequency converted Raman lasers. At present, the blue spectral region is primarily covered by frequency doubled optically pumped semiconductor lasers (OPSLs), or (OPOs) offer Watt level cw output power in the blue spectral regime with continuous tuning ranges of up to 15 nm [16] and more than 50 nm [11], respectively. The wavelength spans of frequency doubled OPSLs are limited, in which aspect the OPOs excel. However, the complexity of the OPOs and their demanding pump source requirements makes them expensive. The intracavity frequency converted Raman laser demonstrated here complements these established laser sources. It excels in simplicity and robustness. Although the emission wavelength of the Raman laser cannot be continuously tuned, it can be configured so that an operator can select between several discrete wavelengths that span the blue spectral region. Further, the use of different Raman transitions in KGW or other Raman crystals will enable spectral coverage to be designed. For example, the selection of smaller Stokes shifts, such as the 89 cm^{-1} Stokes shift of KGW, would create a more closely spaced set of wavelengths, allowing for tuning over a small wavelength range [17] whereas the large

Stokes shift of 1332 cm^{-1} in diamond [18] would create a more widely spaced wavelength set, ranging from blue to yellow.

This research project is financially supported by CNPq: 401580/2012 and FAPESP: 11437-8.

References

1. T. T. Basiev and R. C. Powell, *Opt. Mater.* **11**, 301 (1999)
2. H. M. Pask, *Prog. Quant. Electron.* **27**, 3 (2003).
3. H. M. Pask, *Opt. Lett.* **30**, 2454 (2005).
4. A. J. Lee, D. J. Spence, J. A. Piper, and H. M. Pask, *Opt. Express* **18**, 20013 (2010).
5. A. J. Lee, H. M. Pask, J. A. Piper, H. Zhang, and J. Wang, *Opt. Express* **18**, 5984 (2010).
6. J. Jakutis-Neto, J. Lin, N. U. Wetter, and H. M. Pask, *Opt. Express* **20**, 9841 (2012).
7. D. Geskus, J. Jakutis-Neto, S. M. Reijn, H. M. Pask, and N. U. Wetter, *Opt. Lett.* **39**, 2982 (2014).
8. W. J. Alford, G. J. Fetzer, R. J. Epstein, Sandalphon, N. Van Lieu, S. Ranta, M. Tavast, T. Leinonen, and M. Guina, *IEEE J. Quantum Electron.* **49**, 719 (2013).
9. J. Chilla, Q.-Z. Shu, H. Zhou, E. Weiss, M. Reed, and L. Spinelli, *Proc. SPIE* **6451**, 645109 (2007).
10. S. Calvez, J. E. Hastie, M. Guina, O. G. Okhotnikov, and M. D. Dawson, *Laser Photon. Rev.* **3**, 407 (2009).
11. G. K. Samanta and M. Ebrahim-Zadeh, *Opt. Lett.* **33**, 1228 (2008).
12. D. Geskus, J. Jakutis-Neto, H. M. Pask, and N. U. Wetter, in *Conference on Lasers and Electro-Optics* (2014), paper JW2A71.
13. A. Smith, SNLO, <http://www.as-photonics.com/snlo>
14. A. McKay, O. Kitzler, and R. P. Mildren, *Opt. Express* **22**, 6707 (2014).
15. R. Li, M. Griffith, L. Laycock, and W. Lubeigt, *Opt. Lett.* **39**, 4762 (2014).
16. L. Fan, T.-C. Hsu, M. Fallahi, J. T. Murray, R. Bedford, Y. Kaneda, J. Hader, A. R. Zakharian, J. V. Moloney, S. W. Koch, and W. Stolz, *Appl. Phys. Lett.* **88**, 251117 (2006).
17. M. T. Chang, W. Z. Zhuang, K. W. Su, Y. T. Yu, and Y. F. Chen, *Opt. Express* **21**, 24590 (2013).
18. D. C. Parrotta, A. J. Kemp, M. D. Dawson, and J. E. Hastie, *IEEE J. Sel. Top. Quantum Electron.* **19**, 1400108 (2013).